Available online at www.sciencedirect.com
SCIENCE DIRECT®
Journal of Organometallic Chemistry 689 (2004) 1631–1638
Journal of Organometallic Chemistry
www.elsevier.com/locate/jorganchem

Synthesis, crystal structures and in vitro antitumor activities of some arylantimony derivatives of analogues of demethylcantharimide

Guo-Cang Wang [a], Jian Xiao [a], Lin Yu [a], Jin-Shan Li [a,*], Jing-Rong Cui [b], Rui-Qing Wang [b], Fu-Xiang Ran [b]

[a] State Key Laboratory of Elemento-Organic Chemistry, School of Chemistry, Nankai University, Tianjin 300071, China
[b] National Research Laboratories of Natural and Biomimetic Drugs, Peking University, Beijing 100083, China

Received 25 December 2003; accepted 13 February 2004

Abstract

A series of novel arylantimony derivatives of analogues of demethylcantharimide with the formulae $Ar_nSbL_{(5-n)}$ and $Ar_nSbL'_{(5-n)}$(LH = *N*-hydroxy-demethyldehydrogencantharimide, L′H = *N*-hydroxy-demethylcantharimide, $n = 3, 4$; Ar=C_6H_5, 4-$CH_3C_6H_4$, 3-$CH_3C_6H_4$, 2-$CH_3C_6H_4$, 4-ClC_6H_4, 4-FC_6H_4) were synthesized and characterized by elemental analysis, IR, ^{1}H NMR and mass spectroscopy. The crystal structures of $(C_6H_5)_4SbL$, $(4\text{-}CH_3C_6H_4)_3SbL_2$ and $(3\text{-}CH_3C_6H_4)_3SbL'_2$ were determined by X-ray diffraction. The in vitro antitumor activities of all compounds against six cancer cells are reported.

Keywords: Antimony; Demethylcantharimide; Crystal structures; Antitumor activity

1. Introduction

A substantial number of references describing synthesis and applications of $Ar_nSbX_{(5-n)}$ ($n = 3$, 4; X = halide, alkoxyl, carboxylate, sulphonate, oxime) have appeared in the literature [1–14]. The use of antimony in medicine has been reviewed by Tiekink [15]. Over the last several years, Silvestru co-workers [16–18] reported that some organoantimony (III) derivatives showed significant antitumor activity. In recent years we have found that some organoantimony (V) derivatives exhibit high in vitro antitumor activity [8,9], which is associated with cytostatic activity similar to that of *cis*-platin. However, demethylcantharimide {exo-7-oxabicyclo[2,2,1]heptane-2,3-dicarboximide} and its analogues have also a wide range of biological activity, including antitumor activity [19–21]. In order to investigate whether including the analogues of demethylcantharimide in organoantimony (V) derivatives can improve their antitumor properties we have synthesized a series of arylantimony derivatives of analogues of demethylcantharimide. In addition, we are also interested in studying the nature of bonding and the structure of these compounds.

2. Results and discussion

2.1. Preparations

The title compounds are prepared under anhydrous condition. All compounds are white crystals and stable under ordinary conditions. They are soluble in organic solvents such as dichloromethane, chloroform, acetone and dimethyl sulfoxide, but not soluble in ether, hexane and petroleum ether. The general reaction is shown as follows:

* Corresponding author. Tel.: 00862223504230; fax: 0086222350-3438.

0022-328X/$ - see front matter © 2004 Elsevier B.V. All rights reserved.
doi:10.1016/j.jorganchem.2004.02.015

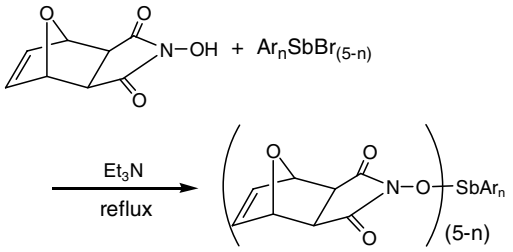

For compounds **I**: $n = 3$, Ar=C_6H_5 (**I_1**), 4-$CH_3C_6H_4$ (**I_2**), 3-$CH_3C_6H_4$ (**I_3**), 2-$CH_3C_6H_4$ (**I_4**), 4-ClC_6H_4 (**I_5**); $n = 4$, Ar=C_6H_5 (**I_6**), 4-ClC_6H_4 (**I_7**).

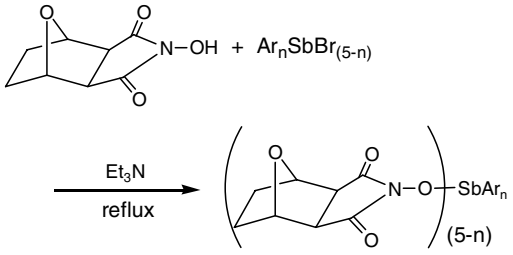

For compounds **II**: $n = 3$, Ar=C_6H_5 (**II_1**), 4-CH_3-C_6H_4 (**II_2**), 3-$CH_3C_6H_4$ (**II_3**), 2-$CH_3C_6H_4$ (**II_4**), 4-ClC_6H_4 (**II_5**), 4-FC_6H_4 (**II_6**); $n = 4$, Ar=C_6H_5 (**II_7**), 4-ClC_6H_4 (**II_8**).

2.2. IR

The IR spectra of these compounds have been recorded in the range of 4000–400 cm^{-1}. The absorption bands can be assigned on the basis of earlier publications and the important data are listed in Table 1.

The IR spectroscopic data provide further support for the molecular constitution of the title compounds. A characteristic feature of five membered ring imides is the presence of bands at about 1785 cm^{-1} (medium) and 1725 cm^{-1}(strong) in the IR spectra of *N*-hydroxydemethylcantharimide [22]. In the IR spectra of the title compounds the absorption vibration frequencies of five membered ring imides are observed in the characteristic regions: a strong absorption due to carbonyl group at 1706–1683 cm^{-1} and a medium absorption due to imine linkage at 1779–1765 cm^{-1}. The absorption vibration frequencies at about 3300 cm^{-1} [22] due to hydroxyl group of free ligands disappeared, indicating the deprotonation of hydroxyl group and formation of Sb–O bond. In addition, the frequencies of Sb–C deformations appear between 453 and 504 cm^{-1}, this is consistent with the literature [1].

Table 1
IR data of the compounds (cm^{-1})

Compound	*v* (C=O)	*v* (C–N–C)	*v* (Sb–C)
I_1	1693 (s)	1768 (m)	457
I_2	1702 (s)	1774 (m)	483
I_3	1698 (s)	1775 (m)	467
I_4	1702 (s)	1776 (m)	504
I_5	1704 (s)	1774 (m)	490
I_6	1683 (s)	1765 (m)	461
I_7	1685 (s)	1770 (m)	490
II_1	1699 (s)	1779 (m)	453
II_2	1702 (s)	1773 (m)	485
II_3	1702 (s)	1774 (m)	468
II_4	1701 (s)	1776 (m)	486
II_5	1706 (s)	1776 (m)	489
II_6	1697 (s)	1778 (m)	473
II_7	1686 (s)	1768 (m)	458
II_8	1686 (s)	1765 (m)	491

2.3. ^1H NMR

The ^1H NMR data of the title compounds are listed in Table 2. The chemical shifts of the protons of the double-bonded carbons (CH=CH) appear between 6.28 and 6.37 ppm, and those of the protons of the single-bonded carbons (CH_2–CH_2) appear between 1.31 and 1.73 ppm. The protons of Ar show a complex multiplet. All the protons in the compounds have been identified and the total number of protons calculated from the integration curve tallies with what was expected from the molecular formula.

2.4. Mass spectra

The main mass spectra data of compound **II_3** are listed in Table 3. In the mass spectra of compound **II_3** the molecular ion peak has never been observed, but the fragment ions found $(M–ONO_3C_8H_8)^+$ (*m/z* 576, 578; intensity 16.2%, 12.0%) and $(ONO_3C_8H_8)^+$ (*m/z* 182; intensity 23.5%) are in agreement with the expected structure of the compound. The breakdown of Sb–O and Sb–C bonds are the main breakdown patterns for the compound.

2.5. Crystal structure

2.5.1. Crystal structure of compound I_6

The colorless crystals of compound **I_6** were obtained from CH_2Cl_2-petroleum ether. One of the approximate dimensions $0.20 \times 0.18 \times 0.14$ mm was mounted in a glass capillary and used for data collection. Fig. 1 shows the molecular structure of the compound and gives the atom numbering scheme. The selected bond distances and angles are listed in Table 4.

The antimony atom of the compound is five-coordinate, the coordination geometry of antimony can be described as a distorted trigonal bipyramid. The three equatorial positions are occupied by the carbon atoms (C(9), C(15) and C(21)) of the three phenyl groups, while the atoms C(27) and O(1) occupy the axial posi-

Table 2
^{1}H NMR data of the compounds

Compound	OCCH	CH–O	CH=CH	CH–CH	Ar
I_1	1.94 (4H, s)	4.92 (4H, s)	6.29 (4H, s)		7.50–8.21 (15H, m)
I_2	1.89 (4H, s)	4.93 (4H, s)	6.28 (4H, s)		7.28–8.05 (12H, m) 2.35 (9H, s)
I_3	1.91 (4H, s)	4.91 (4H, s)	6.28 (4H, s)		7.32–8.03 (12H, m) 2.39 (9H, s)
I_4	2.00 (4H, s)	4.90 (4H, s)	6.28 (4H, s)		7.35–8.44 (12H, m) 2.57 (9H, s)
I_5	2.10 (4H, s)	4.91 (4H, s)	6.32 (4H, s)		7.44–8.12 (12H, m)
I_6	1.94 (2H, s)	4.95 (2H, s)	6.31 (2H, s)		7.42–7.72 (20H, m)
I_7	2.24 (2H, s)	4.96 (2H, s)	6.37 (2H, s)		7.37–7.53 (16H, m)
II_1	1.97 (4H, s)	4.55–4.57 (4H, t)		1.36–1.40 (4H, m) 1.69–1.72 (4H, m)	7.54–8.26 (15H, m)
II_2	1.96 (4H, s)	4.52–4.54 (4H, t)		1.32–1.36 (4H, m) 1.65 (4H, m)	7.28–8.07 (12H, m) 2.38 (9H, s)
II_3	1.98 (4H, s)	4.51–4.52 (4H, t)		1.31–1.37 (4H, m) 1.66–1.69 (4H, m)	7.30–8.01 (12H, m) 2.40 (9H, s)
II_4	2.08 (4H, s)	4.48–4.50 (4H, t)		1.31–1.37 (4H, m) 1.65–1.67 (4H, m)	7.29–8.03 (12H, m) 2.57 (9H, s)
II_5	2.18 (4H, s)	4.50 (4H, t)		1.38–1.41 (4H, m) 1.68–1.73 (4H, m)	7.44–8.10 (12H, m)
II_6	2.16 (4H, s)	4.49–4.50 (4H, t)		1.35–1.42 (4H, m) 1.68–1.71 (4H, m)	7.17–8.21 (12H, m)
II_7	2.04 (2H, s)	4.56–4.57 (2H, t)		1.36–1.41 (2H, m) 1.69–1.71 (2H, m)	7.40–7.71 (20H, m)
II_8	2.34 (2H, s)	4.56–4.57 (2H, t)		1.44–1.46 (2H, m) 1.74–1.77 (2H, m)	7.36–7.50 (16H, m)

Table 3
Fragment ions observed for compound **II_3**

m/z	Fragment	Intensity (%)	*m/z*	Fragment	Intensity (%)
578	$[(3\text{-}CH_3C_6H_4)_3Sb(ONO_3H_8C_8)]^+$	12.0	303	$(3\text{-}CH_3C_6H_4)_2\ Sb^+$	17.4
576	$[(3\text{-}CH_3C_6H_4)_3Sb(ONO_3H_8C_8)]^+$	16.2	214	$(3\text{-}CH_3C_6H_4)Sb^+$	14.4
396	$(3\text{-}CH_3C_6H_4)_3Sb^+$	2.0	212	$(3\text{-}CH_3C_6H_4)Sb^+$	17.6
394	$(3\text{-}CH_3C_6H_4)_3Sb^+$	3.4	182	$(ONO_3H_8C_8)^+$	23.5
305	$(3\text{-}CH_3C_6H_4)_2Sb^+$	10.5	91	$(3\text{-}CH_3C_6H_4)^+$	28.0

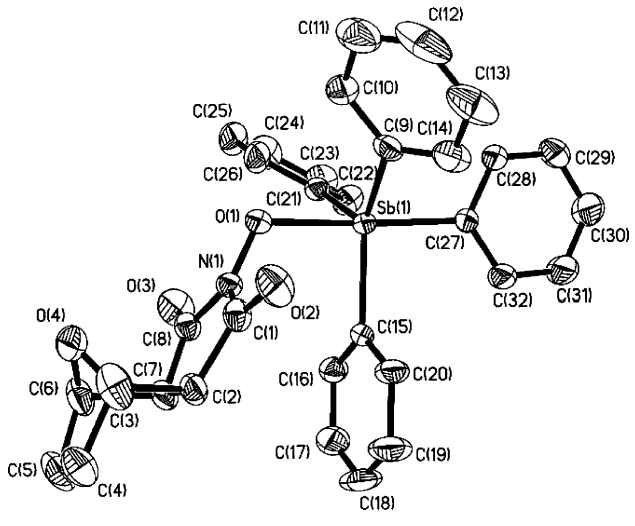

Fig. 1. The molecular structure of compound **I_6**.

tions. The apical Sb(1)–C(27) distance [2.179(6) Å] is slightly longer than the equatorial Sb(1)–C(9), Sb(1)–C(15) and Sb(1)–C(21) distances [2.118(7), 2.112(6) and 2.124(6) Å, respectively]. The Sb(1)–O(1) distance [2.223(4) Å] is longer than the corresponding distance in Ph_4SbOMe [2.061(7) Å] [4], but slightly shorter than that in $Ph_4Sb[ON{=}C(CN)C(O)NH_2]$ [2.259(1) Å] [13].

The Sb(1)–N(1) distance (3.097(8) Å) is obviously shorter than the sum (3.74 Å) of the van der Waals' radii of antimony and nitrogen atoms (2.2 and 1.54 Å, respectively) [23]. This indicates that there is a weak coordination interaction between the no-bonded nitrogen atom and antimony atom, which leads to a small variation of the three equatorial angles of compound **I_6**, the C(9)–Sb(l)–C(15) angle is increased to 125.4(3)°, while the C(9)–Sb(l)–C(21) and C(15)–Sb(l)–C(21) angles are decreased to 119.0(3)° and 113.3(2)°, respectively. The atom Sb(l) is displaced by 0.0674 Å towards C(27) from

Table 4
Selected bond distances and bond angles of compound $\mathbf{I_6}$

Bond	Distance (Å)	Bond	Angle (°)
Sb(1)–C(21)	2.112(6)	C(9)–Sb(1)–C(21)	119.0(3)
Sb(1)–C(9)	2.118(7)	C(15)–Sb(1)–C(21)	113.3(2)
Sb(1)–C(15)	2.124(6)	C(9)–Sb(1)–C(15)	125.4(3)
Sb(1)–C(27)	2.179(6)	C(21)–Sb(1)–C(27)	96.4(2)
Sb(1)–O(1)	2.223(4)	C(9)–Sb(1)–C(27)	93.5(2)
Sb(1)–N(1)	3.097(8)	C(15)–Sb(1)–C(27)	94.8(2)
N(1)–O(1)	1.351(6)	O(1)–Sb(1)–C(21)	87.1(2)
N(1)–C(1)	1.381(8)	O(1)–Sb(1)–C(9)	81.2(2)
N(1)–C(8)	1.396(8)	O(1)–Sb(1)–C(15)	87.4(2)
O(2)–C(1)	1.197(8)	O(1)–Sb(1)–C(27)	174.6(2)
O(3)–C(8)	1.180(8)	O(1)–N(1)–C(1)	122.3(5)
O(4)–C(3)	1.416(10)	O(1)–N(1)–C(8)	122.9(5)
O(4)–C(6)	1.442(9)	C(1)–N(1)–C(8)	114.7(5)
C(2)–C(7)	1.543(10)	N(1)–O(1)–Sb(1)	118.0(3)
C(4)–C(5)	1.303(14)	C(3)–O(4)–C(6)	95.7(6)
C(1)–C(2)	1.496(9)		
C(7)–C(8)	1.494(9)		
C(2)–C(3)	1.555(10)		
C(6)–C(7)	1.549(9)		
C(3)–C(4)	1.469(12)		
C(5)–C(6)	1.496(13)		

the plane defined by the equatorial carbon atoms C(9), C(15) and C(21).

2.5.2. Crystal structures of compounds I_2 and II_3

Both colorless crystals were obtained from CH_2Cl_2-petroleum ether solution. The molecular structures of compounds $\mathbf{I_2}$ and $\mathbf{II_3}$ with the atom numbering scheme are depicted in Figs. 2 and 3, respectively. The selected bond distances and angles of the two compounds are listed in Tables 5 and 6, respectively.

The antimony atoms in compounds $\mathbf{I_2}$ and $\mathbf{II_3}$ are all five-coordinate, and their geometries are represented as a distorted trigonal bipyramid. The Sb–C bond distances [2.101(5), 2.104(4) and 2.110(4) Å in compound $\mathbf{I_2}$,

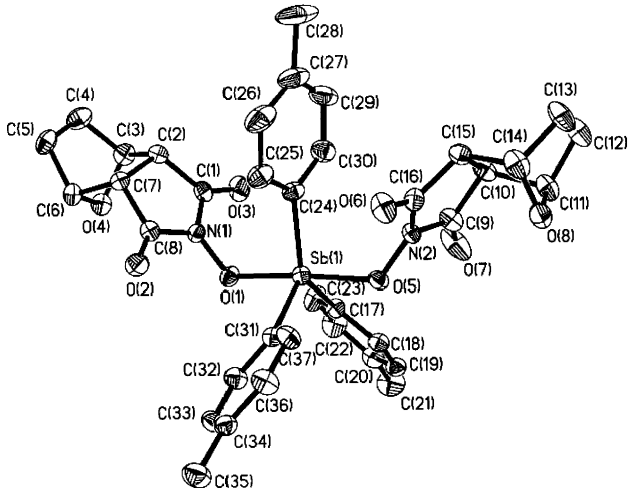

Fig. 2. The molecular structure of compound $\mathbf{I_2}$.

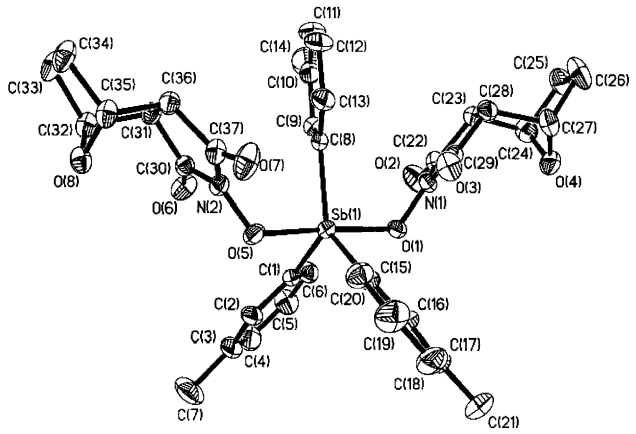

Fig. 3. The molecular structure of compound $\mathbf{II_3}$.

2.109(3), 2.111(4) and 2.113(3) Å in compound $\mathbf{II_3}$] are approximately equal to those in $Ph_3Sb[ON{=}C(Me)C_5H_4N\text{-}2]_2$ [2.098(2) and 2.120(3) Å] [11]. The Sb–

Table 5
Selected bond distances and bond angles of compound $\mathbf{I_2}$

Bond	Distance (Å)	Bond	Angle (°)
Sb(1)–O(1)	2.108(4)	O(1)–Sb(1)–O(5)	176.17(9)
Sb(1)–O(5)	2.119(4)	O(1)–Sb(1)–C(24)	93.89(14)
Sb(1)–C(31)	2.104(4)	O(1)–Sb(1)–C(31)	92.46(15)
Sb(1)–C(24)	2.101(5)	O(1)–Sb(1)–C(17)	86.66(13)
Sb(1)–C(17)	2.110(4)	O(5)–Sb(1)–C(24)	89.93(14)
Sb(1)–N(1)	3.017(5)	O(5)–Sb(1)–C(31)	85.74(14)
Sb(1)–N(2)	3.050(4)	O(5)–Sb(1)–C(17)	91.04(13)
O(1)–N(1)	1.365(4)	C(17)–Sb(1)–C(24)	129.00(15)
O(5)–N(2)	1.357(4)	C(17)–Sb(1)–C(31)	114.92(17)
N(1)–C(8)	1.377(4)	C(24)–Sb(1)–C(31)	116.00(14)
N(1)–C(1)	1.382(4)	N(1)–O(1)–Sb(1)	119.06(18)
C(4)–C(5)	1.306(5)	N(2)–O(5)–Sb(1)	121.2(2)
C(12)–C(13)	1.308(6)		
C(20)–C(21)	1.507(5)		
C(27)–C(28)	1.528(6)		
C(34)–C(35)	1.507(5)		

Table 6
Selected bond distances and bond angles of compound $\mathbf{II_3}$

Bond	Distance (Å)	Bond	Angle (°)
Sb(1)–O(1)	2.106(2)	O(1)–Sb(1)–O(5)	176.16(9)
Sb(1)–O(5)	2.094(2)	O(1)–Sb(1)–C(15)	90.46(13)
Sb(1)–C(8)	2.109(3)	O(1)–Sb(1)–C(8)	89.74(11)
Sb(1)–C(15)	2.111(4)	O(1)–Sb(1)–C(1)	86.91(12)
Sb(1)–C(1)	2.113(3)	O(5)–Sb(1)–C(8)	93.54(11)
Sb(1)–N(1)	3.028(5)	O(5)–Sb(1)–C(1)	93.40(12)
Sb(1)–N(2)	3.027(6)	O(5)–Sb(1)–C(15)	85.87(13)
N(1)–O(1)	1.362(3)	C(8)–Sb(1)–C(15)	131.49(14)
N(1)–C(29)	1.372(4)	C(1)–Sb(1)–C(8)	116.38(14)
N(1)–C(22)	1.373(5)	C(1)–Sb(1)–C(15)	112.07(14)
N(2)–O(5)	1.368(3)	N(1)–O(1)–Sb(1)	120.12(19)
C(25)–C(26)	1.544(7)	N(2)–O(5)–Sb(1)	120.48(19)
C(33)–C(34)	1.537(6)		
C(3)–C(7)	1.515(6)		
C(10)–C(14)	1.514(7)		
C(17)–C(21)	1.507(7)		

O bond distances [2.108(4) and 2.119(4) Å in compound **I_2**, 2.106(2) and 2.094(2) Å in compound **II_3**] are both longer than the corresponding distances in $Ph_3Sb[ON{=}C(Me)C_5H_4N\text{-}2]_2$ [both 2.068(1) Å]. The Sb–N distances [3.017(5) and 3.050(4) Å in compound **I_2**, 3.027(5) and 3.028(6) Å in compound **II_3**] are markedly shorter than the sum (3.74 Å) of the van der Waals' radii of antimony atom and nitrogen atom [23], therefore, there are also weak interactions between Sb(l) and the nitrogen atoms [N(1) and N(2)] in compounds **I_2** and **II_3**.

The C(17)–Sb(l)–C(24) angle in compound **I_2**, which is affected by adjacent N(1) and N(2), is increased to 129.00(15)°, while the C(24)–Sb(l)–C(31) and C(17)–Sb(l)–C(31) angles are decreased to 116.00(14)° and 114.92(17)°, respectively. Correspondingly, the C(8)–Sb(l)–C(15) angle in compound **II_3**, which is also affected by adjacent N(1) and N(2), is increased to 131.49(14)°, while the C(1)–Sb(l)–C(8) and C(1)–Sb(l)–C(15) angles are decreased to 116.38(14)° and 112.07(14)°, respectively. The atoms Sb(l), C(17), C(24) and C(31) in compound **I_2** are coplanar within 0.0130 Å, while the corresponding atoms Sb(l), C(1), C(8) and C(15) in compound **II_3** are coplanar within 0.0115 Å.

2.6. Antitumor activity

The antitumor activities of all compounds are listed in Table 7. The results of bioassay showed that the tetraarylantimony derivatives of analogues of demethylcantharimide have relatively higher antitumor activity against the six cancer cells than the triarylantimony derivatives of analogues of demethylcantharimide. When comparing with cisplatin, the tetraarylantimony derivatives of analogues of demethylcantharimide, namely compounds **I_6**, **I_7**, **II_7** and **II_8**, have very high antitumor activity against some cancer cells. The antitumor activities are also affected by the nature of the aryl at Sb. When Ar is 4-ClC_6H_4 compounds **I_7** and **II_8** have relatively higher antitumor activity.

3. Experimental

Elemental analyses were determined on a Yanaco CHN Corder MT-3 elemental analyzer. IR spectra were recorded on a Bruker Equinox 55 spectrometer in KBr discs. ^{1}H NMR spectra were measured on a Bruker AC-200 spectrometer in $CDCl_3$ solution with TMS as internal standard. Mass spectra were recorded on a VG ZAB-HS mass spectrometer (FAB). All the reactions involving metal halides were carried out under anhydrous. Solvents were purified, dried, and stored by literature methods.

3.1. Reagents

The analogues of demethylcantharimide were synthesized via the following reaction [24,25]. Ar_3SbBr_2 was prepared by the method reported by Lile and Menzies [2], and the solid product was recrystallized from toluene–petroleum ether mixture. To prepare Ar_4SbBr, an adaptation of the method of McEwen et al. [5] was used.

Table 7
Antitumor activity of all compounds in vitro

Compound	Inhibition ratio (%) (10 μg/ml)[a]					
	HL-60	PC-3MIE8	BGC-823	MDA-MB-435	Bel-7402	Hela
I_1	12.1	−1.5	0.6	8.2	10.3	10.8
I_2	17.0	−0.6	1.5	7.3	8.0	6.4
I_3	15.3	−2.2	4.2	6.8	3.2	6.8
I_4	7.6	−6.5	1.5	9.1	7.1	5.4
I_5	18.5	26.2	23.8	3.3	13.3	14.0
I_6	74.5	57.0	65.7	17.5	58.6	6.9
I_7	87.7	84.8	95.8	94.8	97.3	91.1
II_1	−1.7	−20.0	23.7	5.5	1.1	−18.8
II_2	10.4	−1.7	3.8	6.0	12.6	10.8
II_3	−6.7	4.9	22.3	17.4	11.1	−7.0
II_4	8.8	−18.2	16.3	−3.4	6.2	−1.4
II_5	26.8	−15.0	25.3	−9.7	11.2	−0.7
II_6	6.1	6.9	11.2	24.6	1.5	−11.4
II_7	87.6	83.2	83.8	43.7	69.6	38.6
II_8	84.4	71.2	90.7	91.3	92.2	33.6
A	25.4	−16.3	20.2	−0.4	−2.2	−3.5
B	19.3	−11.4	18.6	0.4	6.3	−2.1
C	21.7	−8.2	20.4	1.9	14.3	−3.5
Cisplatin	45.4	76.0	90.6	57.5	33.4	77.7

A: *N*-hydroxy-demethyldehydrogencantharimide, **B**: *N*-hydroxy-demethylcantharimide, **C**: Ph_3SbBr_2.

[a] Inhibition ratio (%) = $(A_1 - A_2)/A_1 \times 100\%$. A_1: the mean optical densities of untreated cells, A_2: the mean optical densities of drug-treated cells.

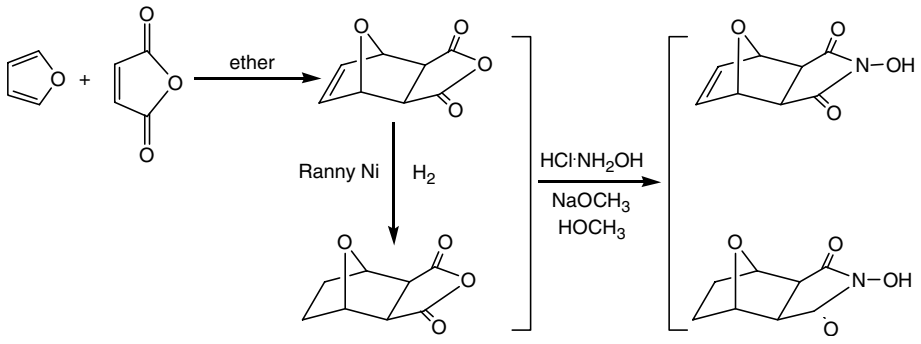

3.2. Synthesis of the title compounds

The title compounds were synthesized by more convenient method. Ar_3SbBr_2 (0.5 mmol) or Ar_4SbBr (1 mmol) was added to a solution of *N*-hydroxy-demethyl(dehydrogen)cantharimide (1 mmol) in 30 ml THF and 0.6 ml Et_3N. The reaction mixture was refluxed for 8 h, cooled and filtered. The filtrate was evaporated in vacuo. The obtained solid was recrystallized from CH_2Cl_2-petroleum ether. The yields, melting points and elemental analysis of the prepared compounds are given in Table 8.

3.3. Crystal structure determination

Diffraction measurements of compounds **I_2**, **I_6** and **II_3** were carried out at 293 K on a Bruker Smart 1000 diffractometer (graphite-monochromatized Mo Kα radiation, $\lambda = 0.71073$ Å). The crystal class, orientation matrix and accurate unit-cell parameters were determined by standard procedures. The intensities were corrected for absorption using SADABS program. The structure was solved by heavy atom method and refined by a full-matrix least square procedure based on F^2. Non-hydrogen atoms were refined with anisotropic thermal parameters. Crystal data are summarised in Table 9.

3.4. Antitumor activities

All cell lines were derived in the National Research Laboratories of Natural and Biomimetic Drugs of Peking University and grown in RPMI 1640 medium with 10% fetal bovine serum, in 5% CO_2 atmosphere.

The antitumor activity was assayed by the MTT or SRB methods [26,27]. The cell lines, human immature granulocyte leukemia (HL-60), human prostatic carcinoma (PC-3MIE8), human gastric carcinoma (BGC-823), human mammary gland carcinoma (MDA-MB-435), human hepatocellular carcinoma (Bel-7402) and human hela carcinoma (Hela) were used for the screening. All cell lines were seeded into 96 well plates at a concentration of about 50 000 cells/ml and were incubated in 5% CO_2 atmosphere at 37 °C for 24 h. Then 20 μl of the sample (organoantimony complex) were added and further incubation was carried out at

Table 8
Yields and elemental analyses of the compounds

Compound	Yield (%)	M.p. (°C)	Elemental analysis: Found (Calc.) (%)			
			C	H	N	Formula for Calc.
I_1	59.2	196 dec	57.33(57.25)	3.84(3.82)	3.74(3.93)	$C_{34}H_{27}N_2O_8Sb$
I_2	72.9	204 dec	54.02(54.31)	3.90(4.20)	3.66(3.33)	$C_{37}H_{33}N_2O_8Sb \cdot CH_2Cl_2$
I_3	58.3	192–193	58.70(58.83)	4.60(4.40)	3.75(3.71)	$C_{37}H_{33}N_2O_8Sb$
I_4	51.7	210 dec	51.15(50.62)	3.81(4.03)	2.93(3.03)	$C_{37}H_{33}N_2O_8Sb \cdot 2CH_2Cl_2$
I_5	63.7	170 dec	50.15(50.00)	3.02(2.96)	3.49(3.43)	$C_{34}H_{24}Cl_3N_2O_8Sb$
I_6	68.9	197 dec	62.96(62.97)	4.39(4.29)	2.40(2.30)	$C_{32}H_{26}NO_4Sb$
I_7	69.5	184 dec	51.22(51.38)	2.95(2.96)	1.96(1.87)	$C_{32}H_{22}Cl_4NO_4Sb$
II_1	77.1	240 dec	57.04(56.92)	4.30(4.36)	4.02(3.90)	$C_{34}H_{31}N_2O_8Sb$
II_2	60.2	274	58.05(58.51)	4.61(4.91)	4.00(3.69)	$C_{37}H_{37}N_2O_8Sb$
II_3	80.4	258–259	58.37(58.51)	4.78(4.91)	3.70(3.69)	$C_{37}H_{37}N_2O_8Sb$
II_4	42.5	280 dec	58.48(58.51)	4.90(4.91)	3.64(3.69)	$C_{37}H_{37}N_2O_8Sb$
II_5	88.9	288	49.76(49.76)	3.53(3.44)	3.44(3.41)	$C_{34}H_{28}Cl_3N_2O_8Sb$
II_6	55.8	272 dec	53.01(52.94)	3.79(3.66)	3.78(3.63)	$C_{34}H_{28}F_3N_2O_8Sb$
II_7	68.6	200 dec	62.64(62.77)	4.46(4.61)	2.33(2.29)	$C_{32}H_{28}NO_4Sb$
II_8	78.7	220	47.55(47.47)	2.92(3.14)	1.99(1.68)	$C_{32}H_{24}Cl_4NO_4Sb \cdot CH_2Cl_2$

Table 9
Crystallographic data for compounds $\mathbf{I_2}$, $\mathbf{I_6}$ and $\mathbf{II_3}$

Compound	$\mathbf{I_2}$	$\mathbf{I_6}$	$\mathbf{II_3}$
Formula	$C_{37}H_{33}N_2O_8Sb$	$C_{32}H_{26}NO_4Sb$	$C_{37}H_{37}N_2O_8Sb$
Temperature (K)	293(2)	293(2)	293(2)
Wavelength (Å)	0.71073	0.71073	0.71073
Crystal system	Triclinic	Monoclinic	Triclinic
Space group	$P\bar{1}$	$P2_1/n$	$P\bar{1}$
Unit cell dimensions			
a (Å)	9.186(15)	9.602(3)	10.307(4)
b (Å)	10.946(18)	12.388(4)	11.461(4)
c (Å)	20.44(4)	25.259(7)	18.335(6)
α (°)	77.42(3)	90	75.405(5)
β (°)	80.88(3)	93.178(5)	89.257(5)
γ (°)	70.56(3)	90(6)	79.731(6)
Volume (Å^3)	1883(6)	2999.8(15)	2061.1(12)
Z	2	4	2
Density (Mg m^{-3})	1.482	1.445	1.497
Absorption coefficient (mm^{-1})	0.928	1.045	0.981
$F(000)$	852	1316	944
Crystal size (mm)	$0.24 \times 0.20 \times 0.18$	$0.20 \times 0.18 \times 0.14$	$0.34 \times 0.22 \times 0.20$
θ Range for data collection (°)	1.03–25.03	1.82–26.42	1.15–26.41
Limiting indices	$-10 \leqslant h \leqslant 10$, $-9 \leqslant k \leqslant 13$, $-24 \leqslant l \leqslant 22$	$-10 \leqslant h \leqslant 12$, $-15 \leqslant k \leqslant 14$, $-20 \leqslant l \leqslant 31$	$-12 \leqslant h \leqslant 12$, $-14 \leqslant k \leqslant 8$, $-22 \leqslant l \leqslant 22$
Reflections collected	7835	16 930	11 918
Independent reflections	6589 ($R_{int} = 0.0244$)	6151 ($R_{int} = 0.0205$)	8353 ($R_{int} = 0.0205$)
Completeness to θ	25.03° (99.4%)	26.42° (99.7%)	26.41° (98.7%)
Absorption correction	Semi-empirical from equivalents	Semi-empirical from equivalents	Semi-empirical from equivalents
Refinement method	Full-matrix least-squares on F^2	Full-matrix least-squares on F^2	Full-matrix least-squares on F^2
Goodness-of-fit on F^2	1.007	1.150	1.019
Final R indices [$I > 2\sigma(I)$]	$R_1 = 0.0353, wR_2 = 0.0717$	$R_1 = 0.0567, wR_2 = 0.1418$	$R_1 = 0.0412, wR_2 = 0.0978$
R indices (all data)	$R_1 = 0.0540, wR_2 = 0.0801$	$R_1 = 0.0970, wR_2 = 0.1628$	$R_1 = 0.0586, wR_2 = 0.1065$,
Largest differential peak and hole (e Å^{-3})	0.468 and −0.419	1.333 and −0.973	0.626 and −0.852

37 °C for 48 h. 50 μl of 0.1% MTT or SRB (Sigma) was added to each well. After 4 h incubation, the culture medium was removed, and 150 μl of isopropanol was added to dissolve the insoluble blue formazan precipitates produced by MTT reduction. The plate was shaken for 20 min on a plate shaker to ensure complete dissolution. The optical density of each well was measured at 570 nm (MTT) or 540 nm (SRB) wavelength. The antitumor activity was determined three times in independent experiments, using three replicate wells per toxicant concentration (10, 1, 0.1 μg/ml) and obtained the mean optical densities for drug-treated cells at each concentration as a percentage of that of untreated cells.

4. Supplementary material

Crystallographic data for the structures reported in this paper have been deposited with the Cambridge Crystallographic Data Centre, CCDC No. 227143 for compound $\mathbf{I_2}$, CCDC No. 227144 for compound $\mathbf{II_3}$ and CCDC No. 227145 for compound $\mathbf{I_6}$. Copies of this information may be obtained free of charge from the Director, CCDC, 12 Union Road, Cambridge, CB2 1EZ, UK (fax: +44-1223-336033; e-mail: deposit@ccdc.cam.ac.uk or http://www.ccdc.cam.ac.uk).

Acknowledgements

We thank that Professor Honggeng Wang and assistant Professor Haibin Song for their support of the Crystallographic study. We are also grateful to professor Kui Wang of National Research Laboratories of Natural and Biomimetic Drugs of Beijing Medical University for testing antitumor activity.

References

[1] G.O. Doak, G.G. Long, L.D. Freedman, J. Organomet. Chem. 4 (1965) 82.
[2] W.J. Lile, R.C. Menzies, J. Chem. Soc. (1950) 617.
[3] A.E. Goddard, J. Chem. Soc. 123 (1923) 2315.
[4] K.W. Shen, W.E. McEwen, L.J. LaPlaca, W.C. Hamilton, A.P. Wolf, J. Am. Chem. Soc. 90 (1968) 1718.
[5] W.E. McEwen, G.H. Briles, B.E. Gidddings, J. Am. Chem. Soc. 91 (1969) 7079.

[6] M.N. Gibbons, D.B. Sowerby, J. Organomet. Chem. 555 (1998) 271.
[7] S.P. Bone, D.B. Sowerby, J. Chem. Res. 82 (1979) 1029.
[8] Y.Q. Ma, J.S. Li, Z.A. Xuan, R.C. Liu, J. Oragnomet. Chem. 620 (2001) 235.
[9] R.C. Liu, Y.Q. Ma, L. Yu, J.S. Li, J.R. Cui, R.Q. Wang, Appl. Organomet. Chem. 17 (2003) 662.
[10] R. Ruether, F. Huber, H. Preut, J. Organomet. Chem. 295 (1985) 21.
[11] A. Gupta, R.K. Sharma, R. Bohra, V.K. Jain, J.E. Drake, M.B. Hursthouse, M.E. Light, Polyhedron 21 (2002) 2381.
[12] V.K. Jain, R. Bohra, R.C. Mehrotra, J. Ind. Chem. Soc. (1980) 404.
[13] K.V. Domasevitch, N.N. Gerasimchuk, A. Mokhir, Inorg. Chem. 39 (2000) 1227.
[14] J. Kopf, G. Vetter, G. Klar, Z. Anorg. Allg. Chem. 409 (1974) 285.
[15] E.R.T. Tiekink, Oncology/Hematology 42 (2002) 217.
[16] C. Silvestru, C. Socaciu, A. Bara, I. Haiduc, Anticancer Res. 10 (1990) 803.
[17] A. Bara, C. Socaciu, C. Silvestru, I. Haiduc, Anticancer Res. 11 (1991) 1651.
[18] C. Silvestru, I. Haiduc, E. Tiekink, D. Devos, M. Biesemans, P. Willem, M. Gielen, Appl. Organomet. Chem. 9 (1995) 597.
[19] A. McCluskey, C.C. Walkom, M.C. Bowyer, S.P. Ackland, E. Gardiner, J.A. Sakoff, Bioorg. Med. Chem. Lett. 11 (2001) 2941–2946.
[20] P.Y. Lin, S.J. Shi, H.L. Shu, H.F. Chen, C.C. Lin, P.C. Liu, L.F. Wang, Bioorg. Chem. 28 (2000) 266.
[21] A. McCluskey, S.P. Ackland, E. Gardiner, C.C. Walkom, J.A. Sakoff, Anticancer Drug Des. 16 (2001) 291.
[22] M. Narita, T. Teramoto, M. Okawara, Bull. Chem. Soc. Jpn. 44 (1971) 1084.
[23] J.A. Dean, Lange's Handbook of Chemistry, 12th ed., McGraw-Hill, New York, 1979, p. 3–120; 3–123.
[24] Y. Liu, Y.Z. Lin, Chin. J. Pharmaceut. 22 (1991) 8.
[25] B. Prager, P. Jacobson (Eds.), Beilsteins Handbuch der Organischen Chemie, 27, Verlag von Julius Springer, Berlin, 1937, p. 260.
[26] P. Skehan, R. Storeng, D. Scudiero, A. Monks, J. Mcmahon, D. Vistica, J.T. Warren, H. Bokesch, S. Kenney, M. Boyd, J. Natl. Cancer. Inst. 24 (1990) 1107.
[27] F. Denizot, R. Lang, J. Immunol. Methods 89 (1986) 271.